Uniform Atomic Layer Deposition of Al_2O_3 on Graphene by Reversible Hydrogen Plasma Functionalization

*René H. J. Vervuurt[1], Bora Karasulu[1], Marcel A. Verheijen[1,2], Wilhelmus (Erwin) M. M. Kessels[1] and Ageeth A. Bol[1]**

[1]Department of Applied Physics, Eindhoven University of Technology, P.O. Box 513, 5600 MB Eindhoven
[2]Philips Innovation Services, High Tech Campus 11, 5656 AE Eindhoven, The Netherlands

1. Plasma treatment reversibility

For the plasma treatments discussed in the main paper, treatment times of 35 and 30s were chosen for the H_2 and O_2 plasma respectively. Longer treatment times led to irreversible damage to the graphene as can be seen in the Raman spectra of Figure S1. After 45 seconds of H_2 plasma treatment the defect related D-band ($1350cm^{-1}$) remains present in the Raman spectrum after ALD deposition and annealing, showing that the functionalization is only partly reversed (Figure S1a). For the O_2 plasma treatments beyond 30s the effect is even stronger, the 2D-peak ($2690cm^{-1}$) almost completely disappears after plasma treatment, and the peaks broaden significantly. The peak-broadening indicates the formation of α-carbon, which can no longer be converted back to graphene in the subsequent ALD and annealing steps. The Hall measurements (Figure S1c) also show that the graphene is irreversibly damaged by the longer plasma treatments. An O_2 plasma treatment of 1min leads to a reduction of the mobility of more than 98% and cannot be recovered after Al_2O_3 ALD and subsequent annealing at 400ºC. After a 45s H_2 plasma treatment the mobility recovers, after ALD and annealing, to only 44% of its original value. Indicating that also in the functionalization process becomes irreversible for longer plasma treatment times, possibly due to ion bombardment damage of the graphene.

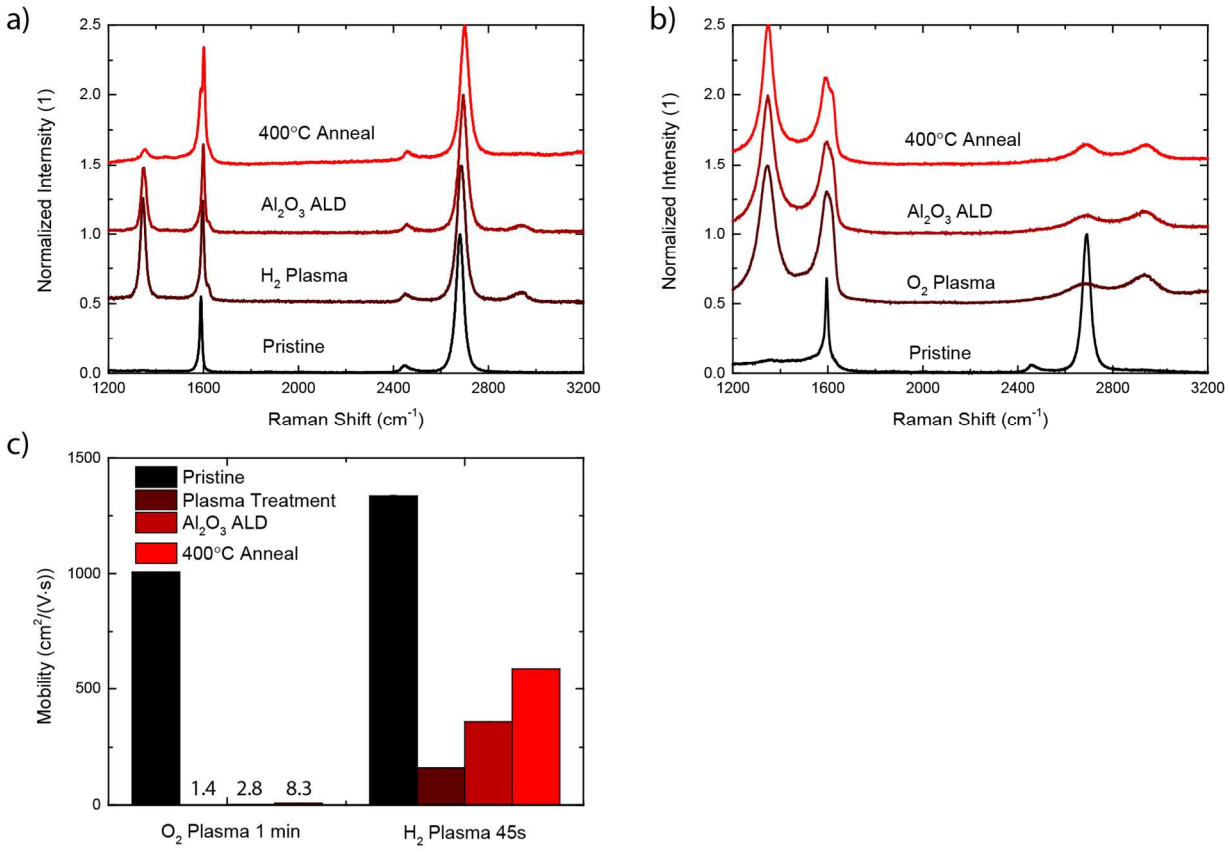

Figure S1: Plasma treatment reversibility as determined by Raman spectroscopy for a) 45s H_2 plasma treated sample and b) 1 min O_2 plasma treated sample and c) the mobility of the samples, after each processing step. The pristine samples were annealed at 400°C before measuring. The ALD was performed at 200°C for 100 cycles.

2. Al_2O_3 coverage on plasma treated graphene as function of the number of ALD cycles

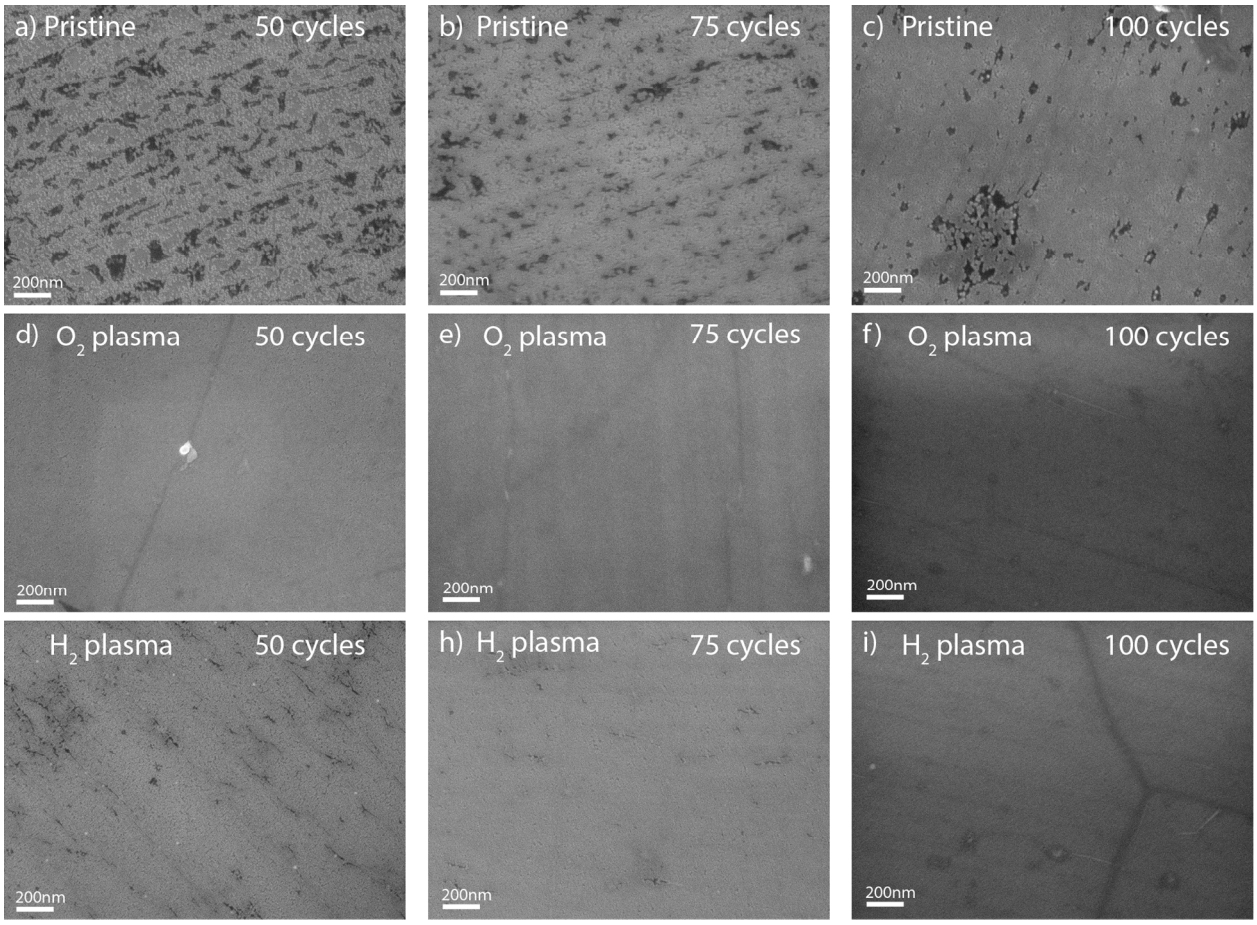

Figure S2: SEM images showing the Al_2O_3 coverage on pristine graphene a,b,c) 30s O_2 plasma treated graphene d,e,f) and 35s H_2 plasma treated graphene for 50, 75 and 100 ALD cycles respectively.

3. Selection of the Simulation Models for Hydrogenated Graphene

For hydrogenated graphene (HG), most theoretical studies have addressed only the double-sided (or fully) HG, viz. graphane (abbreviated here as DSHG), following the original proposition by Sofo et al.[1] Conversely, the single-sided (or semi-)hydrogenated graphene, viz. graphone (abbreviated here as SSHG) was introduced by Zhou et al.[2], but it has attracted considerably less attention possible due to its evidenced tendency to roll up in its free-standing form.[3] Nevertheless, considering that the functionalization of graphene is performed after being placed on a SiO_2/Si support rather than isolated sheets, we use the single-sided form (graphone) in our analysis. Functionalization of either one or both sides of graphene determines maximum amount of functionalities. Relevantly, previous ab initio DFT calculations[4,5] suggested that loading –H functionalities on a single side of graphene becomes energetically highly unfavorable for coverages over 25%. This stoichiometry was confirmed by XPS studies.[6] In contrast, full coverage (C:H ratio being 1) can be achieved for double-sided hydrogenation.

Among the seven different stereoisomers considered for fully hydrogenated graphene (i.e. DSHG), the chair conformation was repeatedly found to be the lowest-energy one (see ref.[7] and references therein), whereas stirrup conformation is slightly less stable (by ca. 0.05 eV). Experimental STM studies recently seconded that DSHG indeed assumes a chair conformation.[8] Likewise, Zhou et al.[2] proposed that graphone (SSHG) is formed in a chair configuration (but with 50% H-adatom coverage), but this form was later shown to be very weak.[7,9] In line with these studies, our DFT calculations predict that hydrogens of graphone can easily leave the surface with a chair decoration upon binding of a TMA precursor. Conversely, a stirrup conformation is predicted to be much more stable, in accord with the preference of H atoms to

form pairs on graphene surface.[7] In addition, an honeycomb configuration was predicted to have the lowest formation energy for graphone (SSHG) with 25% H-loading, and also detected in the STM images of C_4H crystals.[6] Considering the diversity in structure models, we employed the most representative ones with different decoration and coverages for simulating the hydrogenated graphene, as illustrated in Figure S3g,f.

4. Supporting Figures Theoretical Calculations

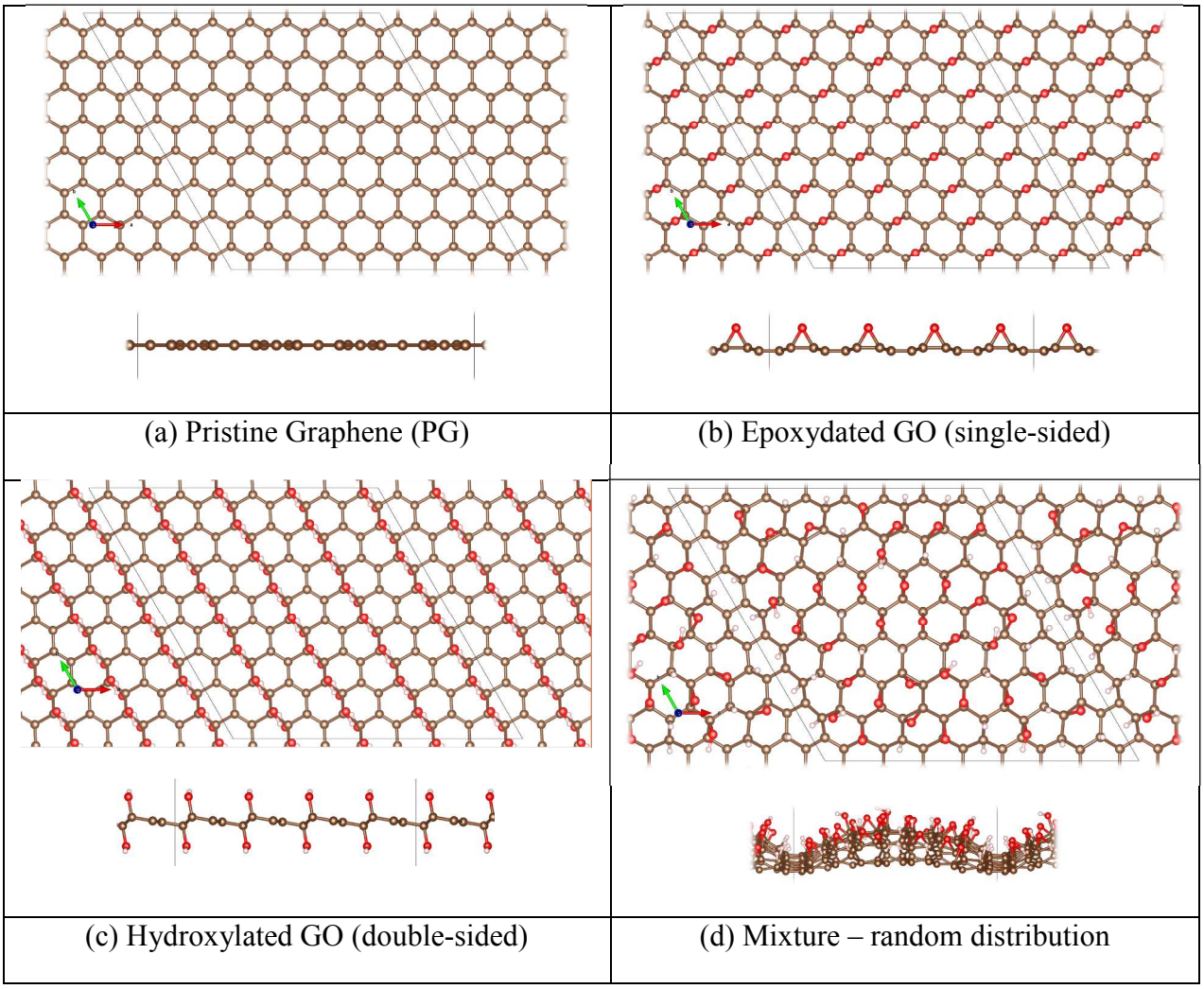

(a) Pristine Graphene (PG)

(b) Epoxydated GO (single-sided)

(c) Hydroxylated GO (double-sided)

(d) Mixture – random distribution

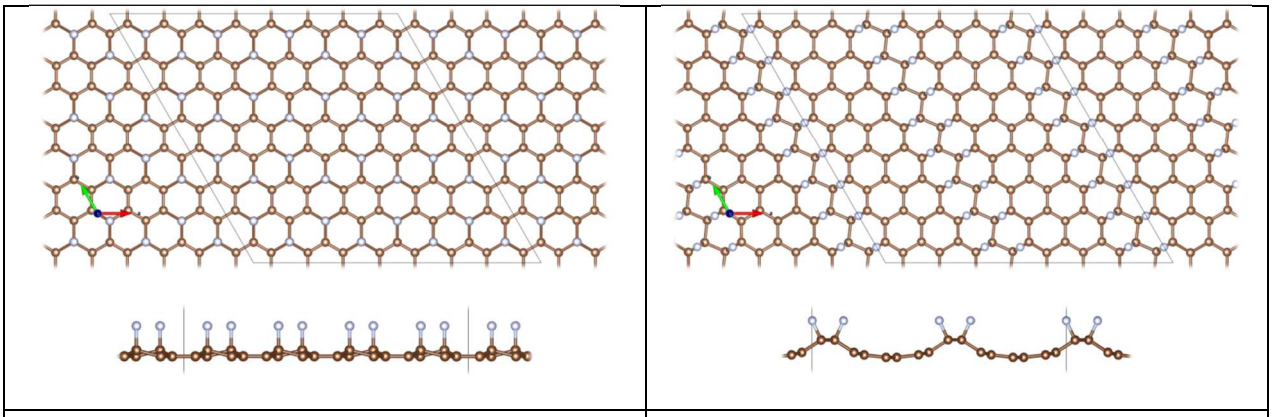

(g) Single-sided Honeycomb (25% coverage)	(f) Single-sided Stirrup (25% coverage)

Figure S3: Ball-and-stick representation of the models (supercells) used for simulating oxygenated and hydrogenated graphene in current DFT calculations. Colour code, C: brown; O: red; H: pink-white.

Pristine (Bare) Graphene

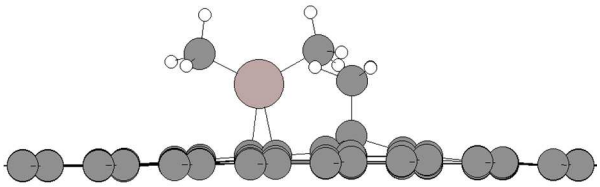

$2\ C^* + AlMe_3 \rightarrow C\text{-}AlMe_2^* + C\text{-}Me^*$

[1.84 eV]

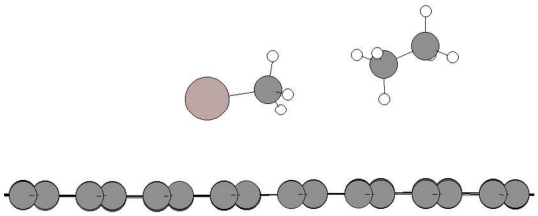

$2\ C^* + AlMe_3 \rightarrow C_2\text{-}AlMe^* + Me_{2\ (g)}$

[0.91 eV]

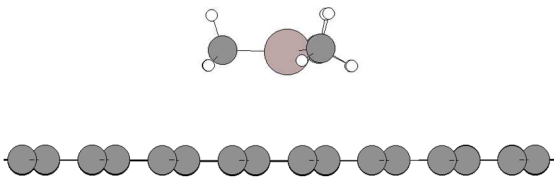

[–0.53 eV]

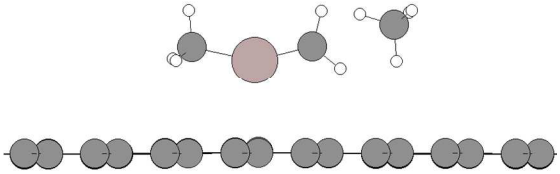

$2\ C^* + AlMe_3 \rightarrow C\text{-}AlMe_2^* + CH_4^*$

[1.92 eV]

Epoxydated GO – Single Sided

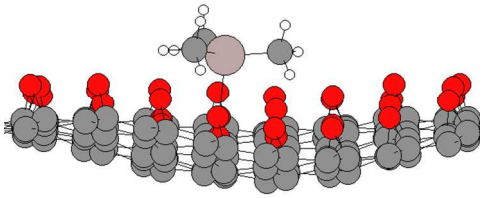

[–1.70 eV]

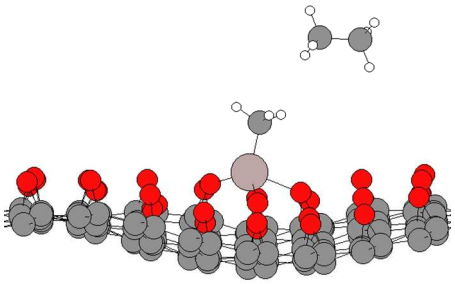

$2(C\text{-}O)^* + AlMe_3 \rightarrow (C\text{-}O)_2\text{-}AlMe^* + Me_{2\ (g)}$

[–7.37 eV]

	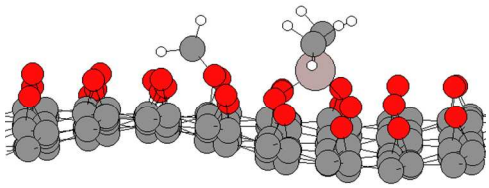 $2(C\text{-}O)^* + AlMe_3 \rightarrow (C\text{-}O)\text{-}\ AlMe_2^* + C\text{-}O\text{-}Me^*$ ΔE_c=-5.69 eV
Hydroxylated GO – Double-Sided	
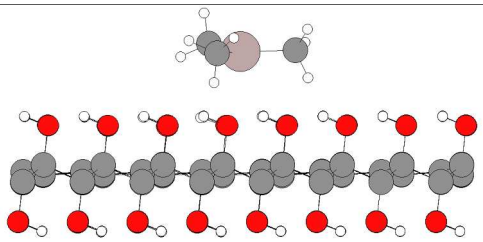 [–0.45 eV]	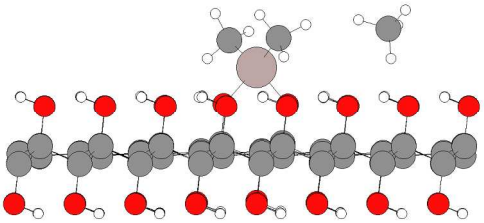 CH_4 [–2.67 eV]
GO Mixture	
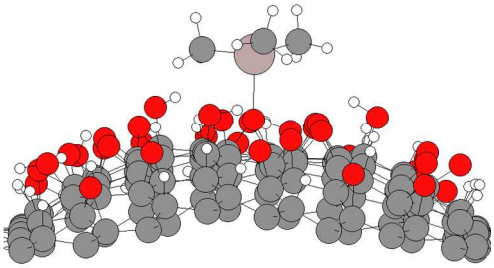 [–0.61 eV]	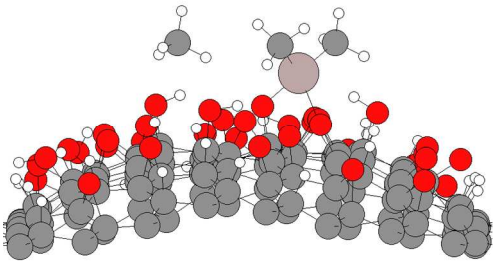 CH_4 [– 3.52 eV]

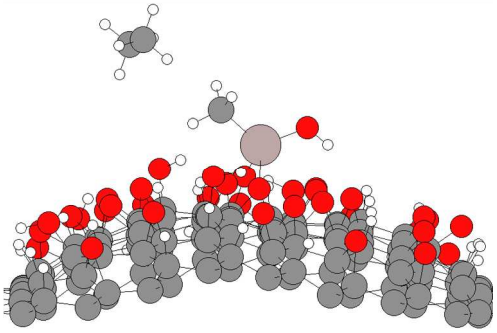

Me_2

[–5.33 eV]

Single-Sided Hydrogenated Graphene (Stirrup Conformation)

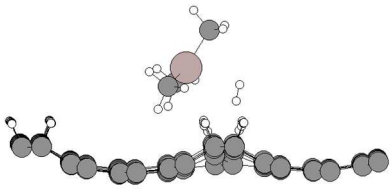

H_2

[–1.29 eV]

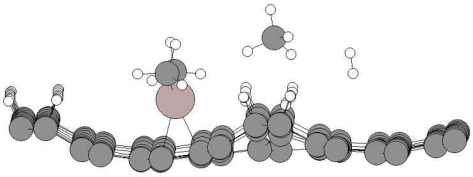

H_2+CH_4

[–2.23 eV]

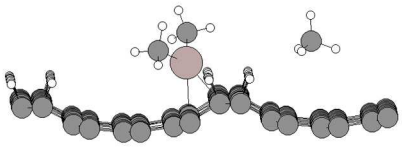

CH_4

[–0.54 eV]

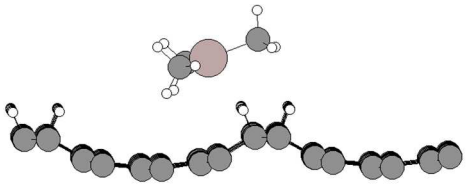

[–0.54 eV]

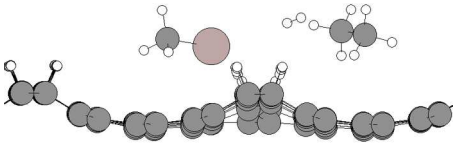

H_2+Me_2

[–0.38 eV]

Single-Sided Hydrogenated Graphene (Honeycomb Conformation)

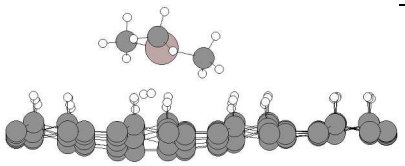

H_2

[–1.00 eV]

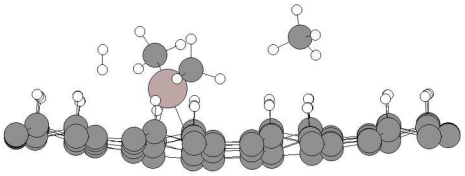

H_2+CH_4

[–1.39 eV]

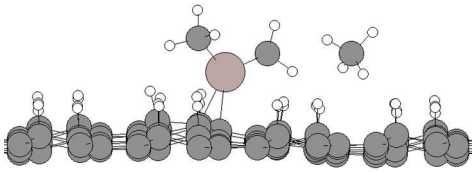

CH_4

[0.12 eV]

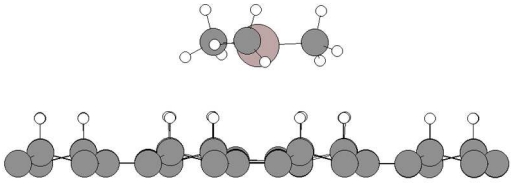

[– 0.44 eV]

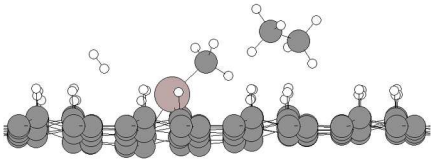

H_2+Me_2

[0.25 eV]

Figure S4: DFT-predicted structures of the lowest-energy (left) physisorbed and (right) chemisorbed species (resulting from different pathways) [and their relative energies] associated with the TMA adsorption on pristine (bare) graphene, oxygenated graphene (i.e. graphene oxide) and hydrogenated graphene surfaces.

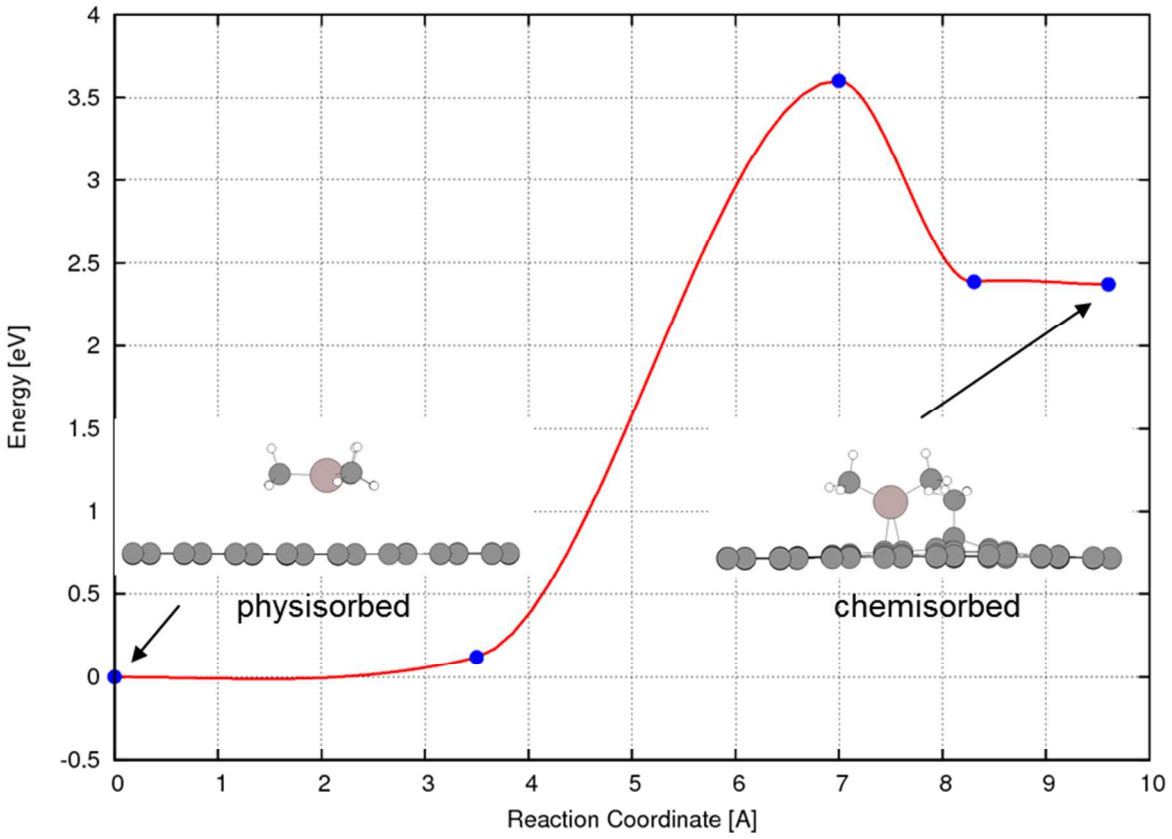

$(C\text{-}C)^* + AlMe_3 \rightarrow C\text{-}AlMe_2^* + C\text{-}Me^*$

$\Delta E_a = 3.60eV$, $\Delta E_r = 2.37eV$.

Figure S5: PBE-D3 level minimum energy paths corresponding to the different reaction pathways for TMA precursor binding on pristine graphene. First and last points on the reaction coordinate correspond to the physisorbed and chemisorbed species, respectively. Physisorbed species is -0.53eV with respect to the separated species (TMA and pristine graphene).

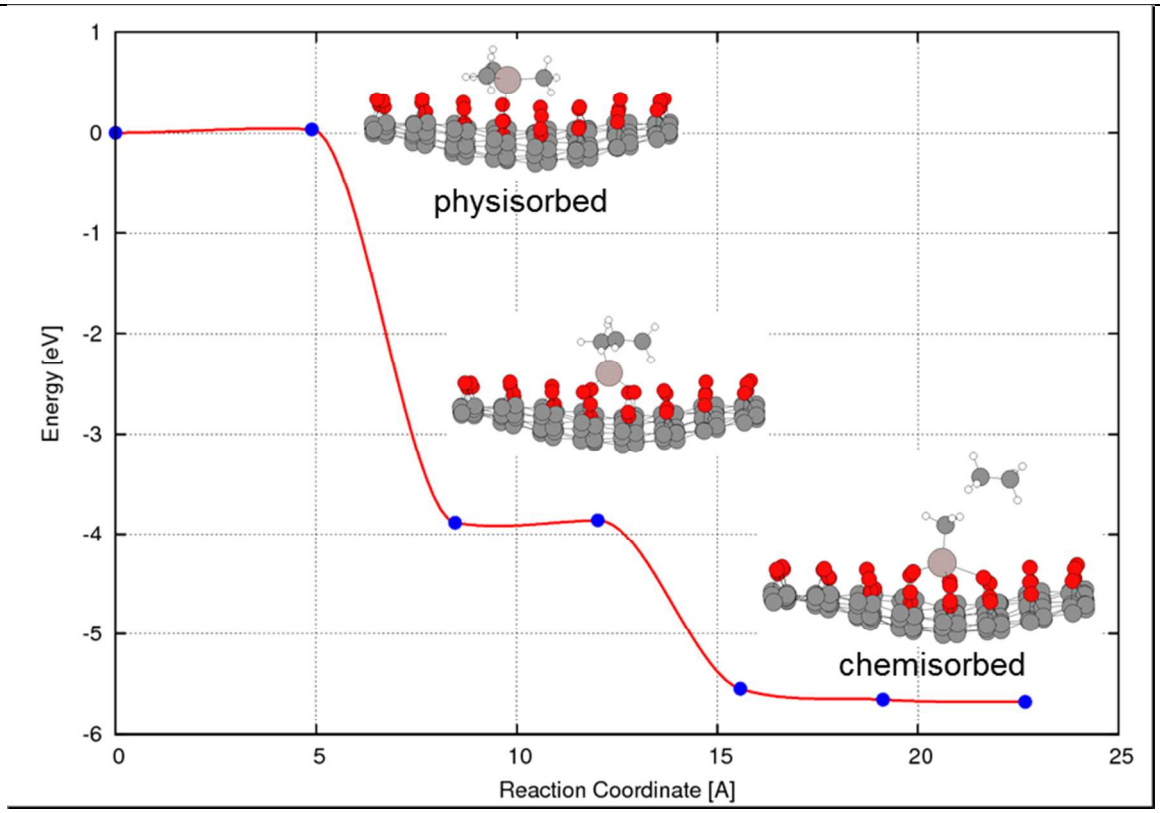

(a) (C-O)* + $AlMe_3$ → (C-O)-AlMe* + $Me_{2\,(g)}$

ΔE_a= 0.04 eV, ΔE_r= -5.67 eV.

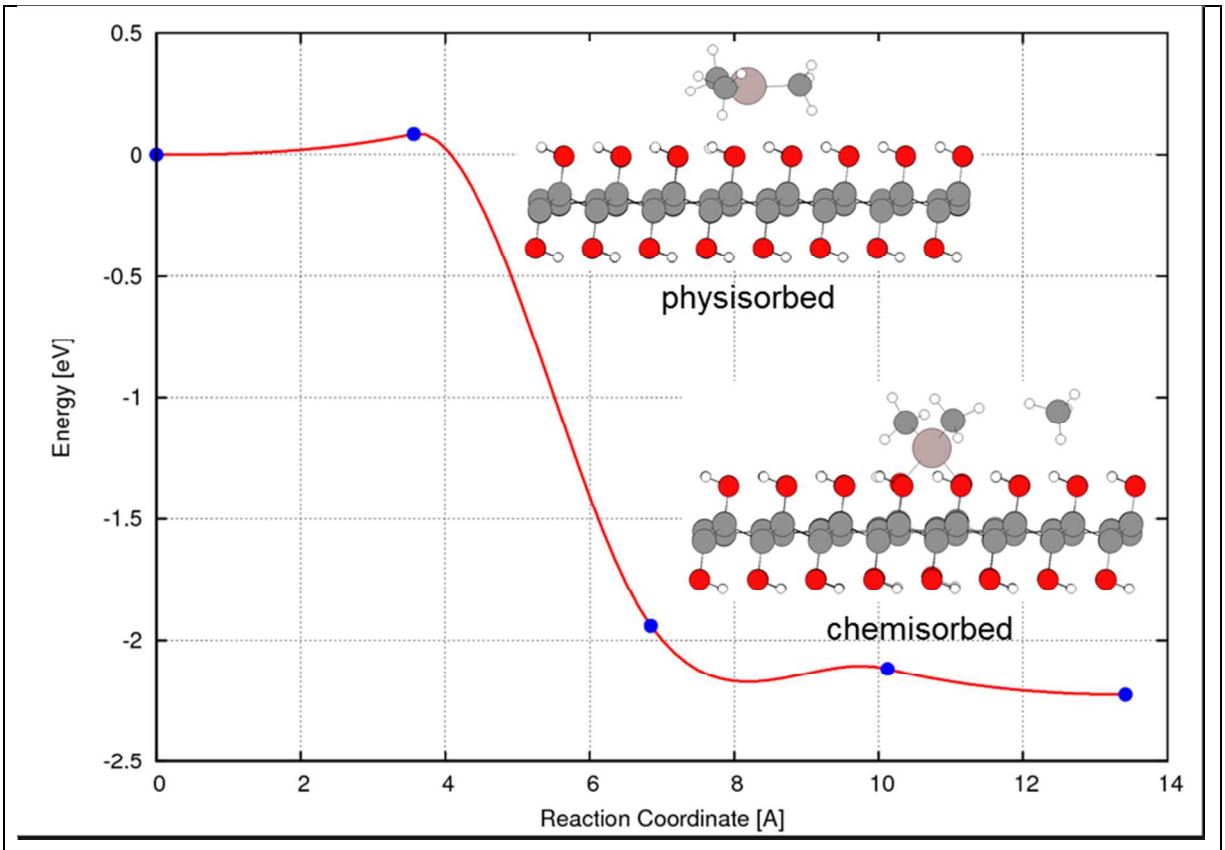

(b) $(C\text{-}OH)^* + AlMe_3 \rightarrow (C\text{-}O)\text{-}AlMe_2^* + CH_{4\,(g)}$

ΔE_a= 0.09 eV, ΔE_r= -2.22 eV.

Figure S6: PBE-D3 level minimum energy paths corresponding to the different reaction pathways for TMA precursor binding on (a) epoxydated and (b) hydroxylated graphene oxide. First and last points on the reaction coordinate correspond to the physisorbed and chemisorbed species, respectively. Physisorbed species of (a) and (b) are -1.70eV and -0.4 eV with respect to the separated species (TMA and epoxydated GO or hydroxylated-GO).

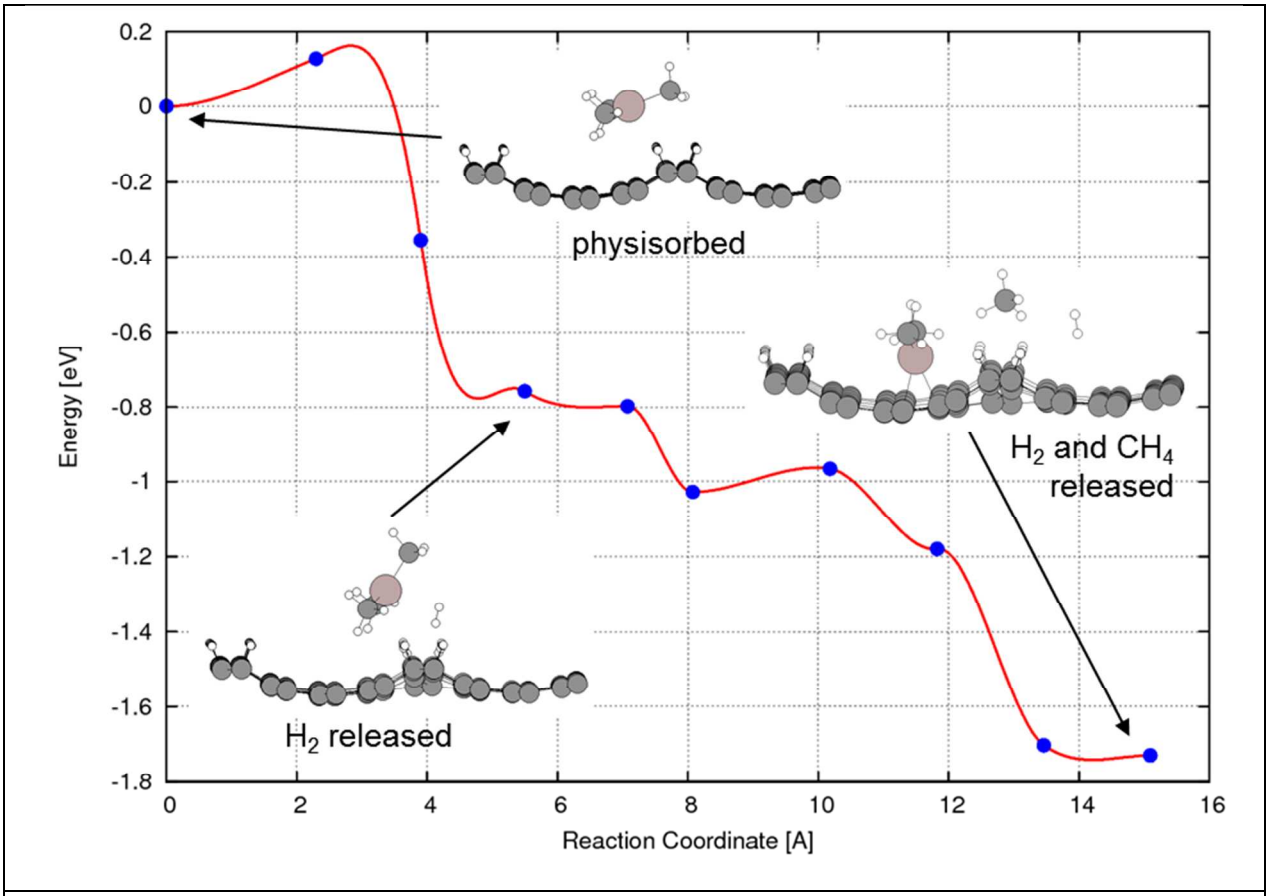

(a) Two-step process (stepwise H_2 and CH_4 release)

(a1) $2(C\text{-}H)^* \rightarrow C\text{-}C + H_{2\,(g)}$

$\Delta E_a = 0.18eV$, $\Delta E_r = -0.75eV$.

(a2) $(C\text{-}H)^* + AlMe_3 \rightarrow C\text{-}AlMe_2^* + CH_{4\,(g)}$

$\Delta E_a = 0.05eV$, $\Delta E_r = -0.89eV$.

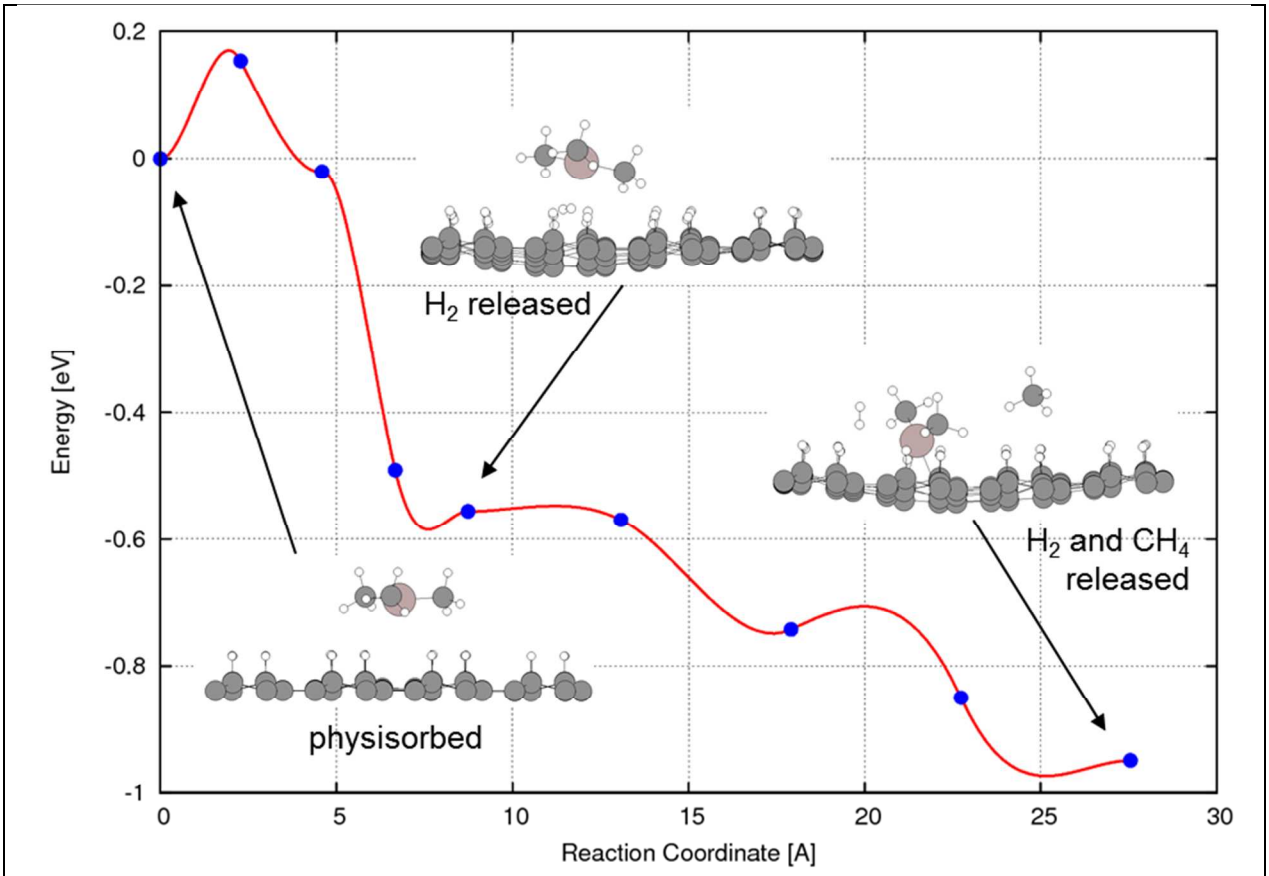

(b) Two-step process (stepwise H_2 and CH_4 release)

(b1) $2(C\text{-}H)^* \rightarrow C\text{-}C + H_{2\,(g)}$

$\Delta E_a = 0.17eV$, $\Delta E_r = -0.56eV$.

(b2) $(C\text{-}H)^* + AlMe_3 \rightarrow C\text{-}AlMe_2^* + CH_{4\,(g)}$

$\Delta E_a = 0.04eV$, $\Delta E_r = -0.38eV$.

Figure S7: PBE-D3 level minimum energy paths corresponding to the different reaction pathways for TMA precursor binding on (a) single-sided stirrup and (b) single-sided honeycomb. First and last points on the reaction coordinate correspond to the physisorbed and chemisorbed species, respectively. Physisorbed species of (a) and (b) and (c) are -0.54eV and -0.44eV with respect to the separated species (TMA and single-sided HG).

5. Effect of the SiO_2 substrate on TMA Binding.

In order to check if the SiO_2 substrate has an effect on the TMA adsorption on pristine graphene, we have considered the hydroxylated α-quartz (001) surface slab model (as discussed in depth in ref.[10]) in our DFT calculations, while keeping the same DFT settings as used for the free-standing graphene case. The resulting DFT energies and corresponding minimum structures are compiled in Figure S8. Evidently, the physisorption energy differs only very slightly (-0.53 eV vs. 0.52 eV) upon the addition of a hydroxylated SiO_2 support. Likewise, for the chemisorption of TMA via the most feasible route involving a methyl transfer, binding energy is affected by the SiO_2 substrate again only insignificantly (1.84 eV vs. 1.82 eV). The rather minute substrate effect can be ascribed to the H-passivation of SiO_2, following from the spontaneous hydroxylation of a freshly-cleaved SiO_2 upon air exposure.[10] This passivation mitigates the strength of the interaction between SiO_2 substrate and graphene, which is mostly through non-bonded interactions rather than bonded ones that fade rapidly with increasing separation of the two subunits.

Free-standing

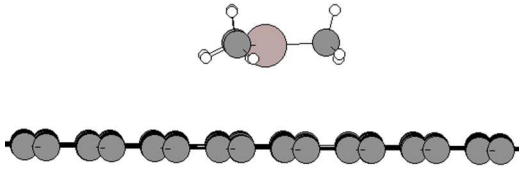

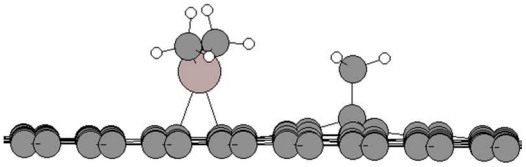

$2\ C^* + AlMe_3 \rightarrow C\text{-}AlMe_2^* + C\text{-}Me^*$

[–0.53 eV] [1.84 eV]

with SiO2 substrate

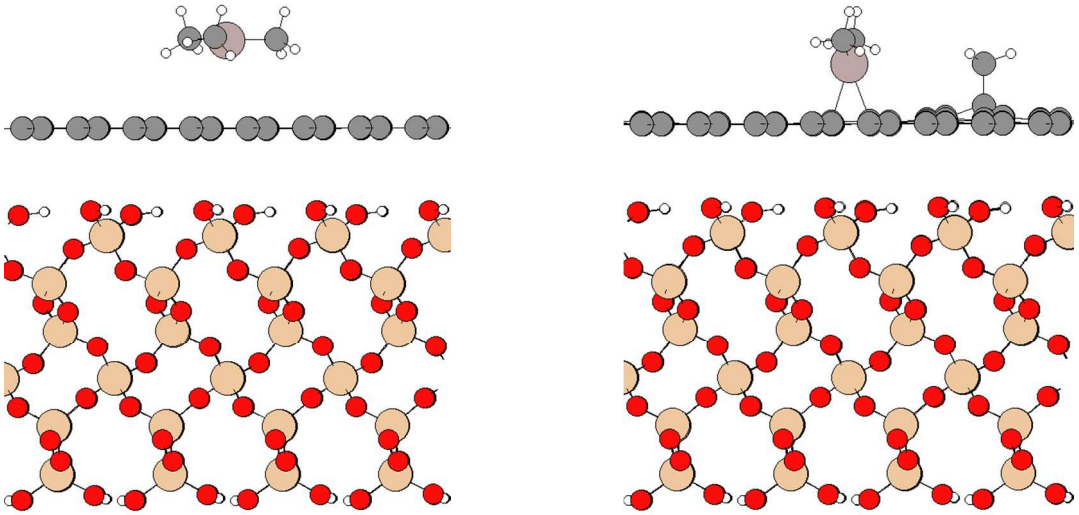

2 C* + $AlMe_3$ → C-$AlMe_2$* + C-Me*

[–0.52 eV] [1.82 eV]

Figure S8. DFT-predicted structures of the lowest-energy (left) physisorbed and (right) chemisorbed species [and their relative energies] resulting from the TMA adsorption on (top) free-standing and (bottom) SiO_2-supported pristine graphene.

REFERENCES

(1) Sofo, J. O.; Chaudhari, A. S.; Barber, G. D. Graphane: A Two-Dimensional Hydrocarbon. *Phys. Rev. B* **2007**, *75* (15), 153401.

(2) Zhou, J.; Wang, Q.; Sun, Q.; Chen, X. S.; Kawazoe, Y.; Jena, P. Ferromagnetism in Semihydrogenated Graphene Sheet. *Nano Lett.* **2009**, *9* (11), 3867–3870.

(3) Neek-Amal, M.; Beheshtian, J.; Shayeganfar, F.; Singh, S. K.; Los, J. H.; Peeters, F. M. Spiral Graphone and One-Sided Fluorographene Nanoribbons. *Phys. Rev. B* **2013**, *87* (7), 75448.

(4) Ewels, C. P.; Van Lier, G.; Charlier, J.-C.; Heggie, M. I.; Briddon, P. R. Pattern Formation on Carbon Nanotube Surfaces. *Phys. Rev. Lett.* **2006**, *96* (June), 216103.

(5) Boukhvalov, D. W.; Katsnelson, M. I.; Lichtenstein, a. I. Hydrogen on Graphene: Electronic Structure, Total Energy, Structural Distortions and Magnetism from First-Principles Calculations. *Phys. Rev. B* **2008**, *77* (3), 35427.

(6) Haberer, D.; Giusca, C. E.; Wang, Y.; Sachdev, H.; Fedorov, A. V.; Farjam, M.; Jafari, S. A.; Vyalikh, D. V.; Usachov, D.; Liu, X.; et al. Evidence for a New Two-Dimensional C 4 H-Type Polymer Based on Hydrogenated Graphene. *Adv. Mater.* **2011**, *23* (39), 4497–4503.

(7) Sahin, H.; Leenaerts, O.; Singh, S. K.; Peeters, F. M. Graphane. *Wiley Interdiscip. Rev. Comput. Mol. Sci.* **2015**, *5* (3), 255–272.

(8) Lin, C.; Feng, Y.; Xiao, Y.; Dürr, M.; Huang, X.; Xu, X.; Zhao, R.; Wang, E.; Li, X.-Z.; Hu, Z. Direct Observation of Ordered Configurations of Hydrogen Adatoms on Graphene. *Nano Lett.* **2015**, *15* (2), 903–908.

(9) Pujari, B. S.; Gusarov, S.; Brett, M.; Kovalenko, A. Single-Side-Hydrogenated Graphene: Density Functional Theory Predictions. *Phys. Rev. B* **2011**, *84* (4), 41402.

(10) Goumans, T. P. M.; Wander, A.; Brown, W. A.; Catlow, C. R. A. Structure and Stability of the (001) α-Quartz Surface. *Phys. Chem. Chem. Phys.* **2007**, *9* (17), 2146–2152.